doi.org/10.52568/001434/JCSP/46.02.2024

Adsorption of Fluoride from Aqueous Solution by Zirconium-Modified Artificial Zeolites: Kinetics, Thermodynamics and Mechanism

Zanen Wu, Xia Chen and Shibiao Wu*

Anhui Province Key Laboratory of Advanced Building Materials, Anhui Jianzhu University, Ziyun Road, 230601, Hefei, Anhui, China.

wsbl@ahjzu.edu.cn*

(Received on 29 August 2023, accepted in revised form 11th December 2023)

Summary: Artificial zeolites (AZ) and AZ modified with zirconium cation (AZZ) were fabricated in this work. AZ and AZZ, which were characterized by SEM and XRD, showed that AZZ was the composite of AZ and ZrO_2. The adsorption kinetics and isotherms of AZ and AZZ towards fluoride removal in water were consistent with the Langmuir and pseudo-second-order models, respectively. AZZ had better fluoride adsorption capacity than AZ. The maximal adsorption capacity of fluoride onto AZZ reached up to 128.2 mg/g. Moreover, the thermodynamic studies illustrated that the adsorption procedure was spontaneous and endothermic. The effect of solution pH on AZZ fluoride adsorption was also investigated, and the results showed that the more acidic the fluoride solution, the better the fluoride adsorption capacity. After five cycles of regeneration, the adsorption capacity of AZZ was maintained at 78 %. Based on zeta potential measurements, this work proposed that the electrostatic attraction between AZZ and fluoride ions (F^-) should be the mechanism for F^- adsorption onto AZZ in water.

Key words: Zeolite; Adsorption; Fluoride; Kinetics; Thermodynamics.

Introduction

Fluorine is known as one of the micronutrients that is crucial towards human health [1]. It plays a pivotal position in the prevention of dental cavities and osteoporosis. However, excessive ingestion can lead to the weakening of bones, osteosynthesis of ligaments and tendons, along with unusual growth of the human and animal skeletal system, which is referred to as skeleton fluorosis [2]. Drinking water containing high fluoride content for a prolonged time can accumulate and result in cancer, and osclerosis (fragile bones and calcification of the ligaments), which indicates an impaired function of the neurologic system in a person [3]. Therefore, the World Health Organization (WHO) recommended the fluoride level in daily drinkable water should not surpass 1.5 $mg \cdot L^{-1}$ [4].

In order to effectively eliminate the redundant fluoride in contaminated water, numerous studies have been conducted recently to develop defluoridation technologies[5]. These include chemical deposition [6], adsorption [7], coagulation [8], nano filtration [9], electrodialysis [10], ion-exchange method [11], among others. The adsorption method is known to have several advantages such as easy operation, high removal ability, cost effectiveness and reusability [12]. Currently, various adsorbents, including activated alumina [13], ion exchange resin [14], activated carbon [15], and oxides containing rare earth metals [16], magnetic-chitosan [17] and bauxite nano scale composites [18], have been utilized for defluorination.

As environmental remediation materials, zeolites have attracted wide attention[19]. In general, zeolites are made of silica and alumina tetrahedrons, and the tetrahedrons are gradually transformed into unitary rings, bimodal rings, and poly cycles to build a three-dimensional spatial shelf-like crystalline polyhedral cage structure. Zeolites are suitable adsorbents because of their huge specific surface areas.

In this work, synthetic zeolite was produced using a hydrothermal process and then modified with zirconium cations. The fluoride adsorption ability, isotherm and kinetic studies of AZZ in water were

*To whom all correspondence should be addressed.

examined. The influence of temperature and pH on fluoride adsorption were also studied.

Experimental

Materials

Nano silicon dioxide (SiO_2 , 99.5% metal-based, 15nm, Aladdin), nitric acid (HNO_3,65%,AR), sodium hydroxide (NaOH, AR), sodium fluoride (NaF, AR), sodium aluminate ($NaAlO_2$, AR, Macklin), alum ($KAl(SO_4)_2$•$18H_2O$,AR), Ultra-pure water (18 MΩ•cm) was manufactured by PSDK System (ZIHANSHIJI, Beijing, China) and Zirconium chloride($ZrCl_4$, AR) were acquired from China National Pharmaceutical Group Corporation.

Preparation and modification of zeolites

Preparation of artificial zeolite

NaOH *(*2.67 g), $NaAlO_2$ (0.7798 g), SiO_2 (1.715 g) and ultrapure water (25 mL) were combined and agitated at 800 rev/min by a rotary magnetometric stirrer for 12 hr till a homogeneous white gel was attained. The white gel was then moved to an autoclave and heated at 105 °C for 24 hr. The white sediment was generated in the autoclave, whereas, the supernatant liquid was discarded. The sediment from the centrifugation washed by ultra-pure water several times till the pH value of the supernatant was in the range of 7 and 8. The sediments were then powdered to AZ by drying in an oven at 65 °C for 24 hr.

Modification of the zeolite

At a ratio of 10 mL solution to 1 g powder, the artificial zeolite powder and 0.1 mol/L zirconium chloride solution were mixed in a sealed glass cup at room temperature for a week, and a hydrogel was subsequently produced. Afterwards, the hydrogel was soaked in 2000 mL ultra-pure water for 24 h to wash away the excess ions. The water was replaced by fresh ultra-pure water, and the washing operation steps above were repeated five times. Subsequently, the purified hydrogel was lyophilized. The frozen dried powder was heated at 2 °C/min to 600 °C in air by an annealing oven. After 4 hr, the powder was naturally cooled in the oven to room temperature. Finally, the AZZ product was obtained.

Characterization

X-ray diffractometer (X'Pert PRO) measurements were performed using a Cu Ka resource (A=1.541 Ä). The powder morphology was studied by field emission scanning electron microscopy (Regulus 8100, Hitach, Japan) operating at 5 or 15 kV.

Experimental procedures

Aqueous fluoride solutions were obtained by solubilizing NaF in ultrapure water as a simulated fluoride-contaminated water. The preliminary fluoride values were regulated to the pH value desired by adding 0.1 M NaOH or HNO_3 aqueous solution. pH values were measured by a Rex pH meter (PHB-4, Shanghai, China).

Adsorption kinetics experiments

A 100 mL 3 ppm (mg/L) fluoride solution was compounded with the proper quantity of adsorbent in a hermetically closed 250 mL plastic conical flask and stirred with an electromagnetic stirrer (800 revolutions per minute) for 24 hr at 298 K. The proportion of adsorbent mass (m) to solution volume (v) was *m*/*v* = 1 and 2 g/L, respectively. During the experiment, the samples were gathered from the mixture at periodic times and were separated using injector-driven filters (0.22 μm). The fluoride consistency in both the initial solution and the transparent liquid after filtration were measured by means of a selective fluorinated ion electrode.

Adsorption isotherms experiments

The same quantity of aqueous fluoride solutions of diverse fluoride concentrations were combined with the appropriate amount of sorbent in sealed plastic vials and shaken with an oscillator at 170 rpm for 24 h at 293, 313 and 333 K. The ratio was *m*/*v* = 1 g/L. Fluoride primary and ultimate levels were examined as described previously. The adsorption rate and distribution coefficient (K_a) were computed using the formula below:

$$Adsorption(\%) = \frac{(C_0 - C_e)}{C_0} \times 100\% \quad (1)$$

$$Q_e = (C_0 - C_e) \times \frac{\mathrm{v}}{\mathrm{m}} \quad (2)$$

$$K_a = \frac{(C_0 - C_e)}{C_0} \times \frac{\mathrm{v}}{\mathrm{m}} \quad (3)$$

where C_0 is the original concentration (mg/L), C_e is the equilibrium concentration (mg/L), m (g) is the adsorbent mass, v (mL) is the volume of the suspended solution, and Q_e (mg/g) is the equilibrium volume of adsorption.

pH influence experiments

The influence of pH on fluoride adsorption was investigated by the use of 14 ppm fluorine solution and 1 g/L adsorbent at various pH values and 298 K experimental temperature. The experimental apparatus and adsorbent were tested for adsorption volume as in the previous experiments.

Adsorbent regeneration experiments

The experimental procedure was as follows: 200 mg raw adsorbent and 20 ppm fluoride ion solution were prepared in a closed plastic cone vial, where *m/v* =1 g/L; and then oscillated for 12 hr at 25 °C and 170 rpm. The sampling and fluorine concentration were measured in the same way as the preceding ones. Following sampling, the remaining compound was centrifuged and once rinsed with a 10-fold volume of deionized water to the volume of the precipitate. The precipitate was then homogeneously combined with the regenerant (i.e., a saturated alum solution 10 times the volume of the precipitate) for one min and rinsed by centrifugation with deionized water till the pH value ranged from 6 to 7. The regenerated adsorbent was dried as indicated in section 2.2. Following desiccation, the subsequent stages of fluorine adsorption and recycling were effective until the fifth cycle.

Results and Discussion

Adsorbent characterization

X-ray Diffraction (XRD)

Fig. 1 displays the XRD patterns of AZ, AZZ, standard PDF cards of zeolite (No. 38-0240) and zirconium dioxide (No. 83-0940). The AZ pattern is in very good agreement with the NO.38-0240 standard card, proving that zeolite was synthesized successfully in this work. Except for the peak (111) of zeolite at 6.2 degrees, which becomes very weak in the AZZ pattern, the largest number of AZ peaks such as (331), (533) and (751) remain in AZZ. This proves that the compositions of zeolite remain in AZZ after annealing. Another intense peak (-111) appears in the AZZ pattern at 28.2 degrees, which is consistent with the strongest peak in PDF card No. 83-0940 implying that zirconium dioxide formed in AZZ after annealing. Therefore, the AZZ prepared in this paper is a composite of zeolite and zirconium dioxide.

SEM Analysis

The forms of the AZ and AZZ were observed by SEM analysis. The AZ grains are illustrated in Fig. 2(A). As observed, the dimension of the AZ particles was in the micrometer scale with a diameter of approximately 0.5 μm. The shape of the grains was similar to a pyramid, and the grains were gathered and formed clusters that were similar to flowers. The large number of small spherical particles in Fig. 2(B) were tightly attached to the AZ grains. Considering the peaks of zirconium dioxide in the AZZ XRD patterns, the small spheres were attributed to zirconium dioxide formation.

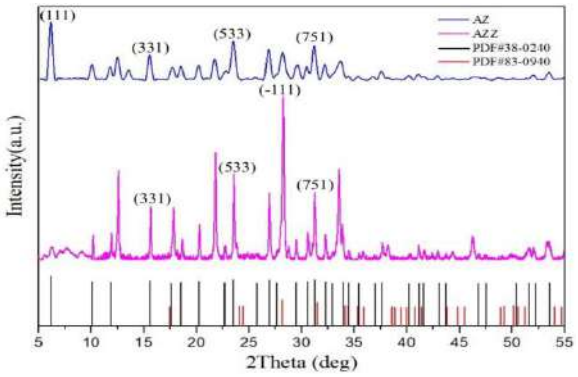

Fig. 1: XRD patterns of AZ, AZZ.

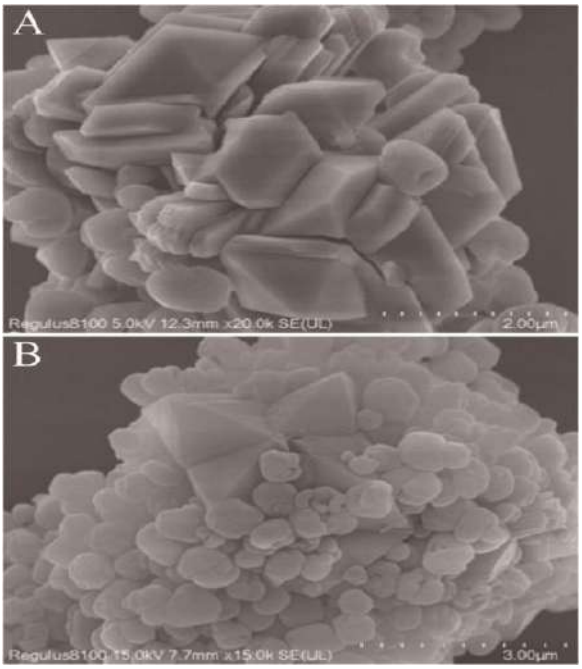

Fig. 2: SEM images of (A) AZ, (B) AZZ.

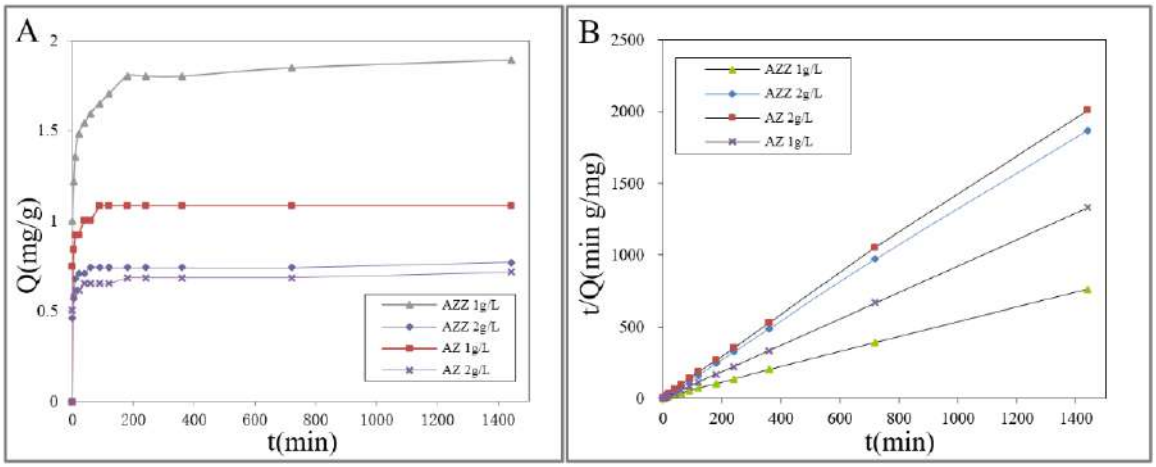

Fig. 3: Adsorption kinetic curve(A) and quasi-second-order kinetic model(B). $[F^-]_{initial}$ =3ppm, Initial pH=6.5, 298K.

Batch adsorption kinetics

Adsorption kinetics tests were conducted by batch experiments. The original fluoride concentration ($[F^-]_{initial}$), temperature and pH were 3 ppm, 298K and 6.5, respectively. The proportion of adsorbent mass (m) to solution volume (v) was m/v = 1 or 2 g/L. The reaction time, t (min) is shown on the horizontal axis, while the F^- adsorption capacities, Q (mg/g), is represented on the vertical axis. The adsorption of F^- on the zeolite was rapid during the first 20 minutes and then slowed down. The fast adsorption may be explained by the rapid translocation of F^- to the adsorbent particle surface, whereas the subsequent sluggish adsorption is accounted for by the progressive spreading of F^- into the intraparticle pore spaces within the adsorbent[20]. Based on Fig. 3(A), the adsorption capacity measured at m/v = 1 g/L was found to be better than that measured at m/v = 2 g/L.

The adsorption kinetic data were analyzed using a pseudo-second-order kinetics model in keeping with the supposition that chemisorption was the procedure that determines the rate of adsorption. The pseudo-second-order kinetic model can be summarized by equation (4):

$$\frac{t}{Q} = \frac{1}{Q_e} t + \frac{1}{k_2 Q_e^2} \quad (4)$$

where k_2 (g mg^{-1} min^{-1}) is the pseudo-second-order rate constant. Q_e and Q are the F^- adsorption capacity at equilibrium and time (t), respectively. The values of Q_e and k_2 can be derived by graphing t/Q against t. The preliminary adsorption rate, r_0 (mg g^{-1} min^{-1}) can be derived from equation (5):

$$r_0 = k_2 Q_e^2 \quad (5)$$

Fig. 3 (B) illustrates the link with t/Q and t, and the linear fitting of t/Q vs t data. The parameters Qe (mg/g), k_2, r_0 (g mg^{-1} min^{-1}) and R^2 (coefficient of determination) obtained after linearity registration of the data sites are shown in Table-1.

The R^2 (coefficients of determination) in Table-1 are all extremely near to 1, which means that the capture of F^- by the adsorbent fits well with the pseudo-second-order kinetics model.

Table-1: Rate constants and correlation coefficients of the pseudo-second-order kinetic models.

Adsorbents	m/V (g/L)	Q_e (mg/g)	k_2 (g mg^{-1} min^{-1})	r_0 (mg g^{-1} min^{-1})	R^2
AZ	1	1.08	0.589	0.692	1.000
	2	0.72	0.200	0.102	1.000
AZZ	1	1.89	0.0575	0.205	1.000
	2	0.77	0.2734	0.162	1.000

Adsorption isotherms

Fig. 4 exhibits the adsorption isotherms for fluoride in water on AZ and AZZ at 298 K. The isotherms can depict the dependence of the residual fluorine concentration in solution and the quantity of fluoride adsorbed.

There are many different types of adsorption isotherms, of which the Freundlich models and Langmuir [21-22] are the most commonly utilized.

The most significant monolayer adsorption model was developed by Langmuir [22]. The basic hypothesis of Langmuir adsorption theory is that adsorption occurs at a particular uniform location inside the adsorbent [23]. In contrast to other adsorption theories, the strength of the Langmuir theory (or equation) is that it provides a maximal amount of adsorption. The Langmuir isotherm module can be summarized in equation (6):

$$Q_e = \frac{Q_m K_L C_e}{1+K_L C_e} \quad (6)$$

where *Ce* is the equilibrium concentration of F^- in aqueous solution ($mg \cdot L^{-1}$). *Qe* is the volume of F^- adsorbed on adsorbents ($mg \cdot g^{-1}$). Q_m is the maximal amount of F- adsorbed for every unit of sorbent weight to develop a perfect single-layer covering on its surface. K_L denotes the proportion of the sorption and desorption rate constants, which should be varied with the change in temperature. According to the experimental points, Langmuir model curves (solid lines) were fitted and plotted in Fig. 4.

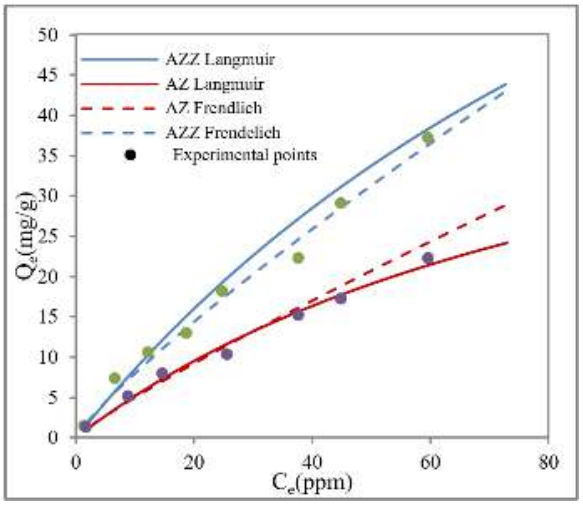

Fig. 4: Langmuir and Freundlich isothermal model of two types zeolite. Original m/v=1g/L, pH=6.5,298K.

The Freundlich model is applied to assume that the adsorption process occurs on a dissimilar surface and that the adsorption process varies with surface covering. The Freundlich isotherm model can be depicted in equation (7):

$$Q_e = K_F C_e^{1/n} \quad (7)$$

where K_F and n are the Freundlich coefficients associated with the adsorption volume and adsorption strength, correspondingly. Freundlich model fit curves (dashed lines) were also plotted in Fig. 4.

The parameterizations of the Langmuir and Freundlich models are presented in Table 2. The coefficients of determination (R^2) of the Langmuir and Freundlich models for AZ are 0.9991 and 0.9859, respectively, and for AZZ are 0.9946 and 0.9545, respectively. Because the R^2 values of the Langmuir models are closer to 1 than the R^2 values of the Freundlich models, this indicates that the Langmuir model is a more favorable description of F^- on AZ and AZZ than the Freundlich model, demonstrating that F^- adsorption on the zeolites was single-layer covering. In the Langmuir model, the maximum value Q_m of fluoride adsorption on AZZ is 128.2 $mg \cdot g^{-1}$, which showed an excellent performance. According to Table-2, the *Qm* of AZZ is 1.24 times as high as that of AZ, which proves that the strategy of Zr modification of AZ was successful.

Table-3 shows the different adsorption effects of zeolite materials prepared by various modification methods on inorganic fluorine in water[24-26] and the comparison with zirconium-modified zeolites. As shown in Table-3, the adsorption performance of AZZ was much improved than that of bare-zeolite, and the its performance was outstanding among different modified zeolites.

Effect of temperature on AZZ adsorption for fluoride in water

This work examined the impact of temperature on the adsorption of fluoride in water by AZZ. The initial pH was 6.5, and the dose of AZZ was 1 g/L. Three thermodynamic experiments were performed at 293, 313 and 333 K. The outcomes are presented in Fig. 5.

Table-2: Parameters for Langmuir and Freundlich models of F^- adsorption on adsorbent.

Adsorbents	Langmuir $Q_e = \frac{Q_m K_L C_e}{1 + K_L C_e}$			Freundlich $Q_e = K_F C_e^{1/n}$		
	Q_m(mg/g)	K_L(L/mg)	R^2	K_F(mg^{1-n}L^n/g)	n	R^2
AZ	57.8	0.009887	0.9991	0.6518	1.131	0.9859
AZZ	128.2	0.007153	0.9946	1.1388	1.181	0.9545

Table-3: Fluoride sorption on different zeolite materials.

Adsorbent	Experimental condition	q_m/(mg·g^{-1})	reference
Bare-zeolite	298K	-	[1]
$CaCl_2$-modified zeolite	pH=6,298K	2.23	[1]
Fe^{3+}-modified zeolite	pH (6.7±0.3), room temperature, aqueous solutions, concentration: 5−40 mg/L	2.31	[24]
La-zeolite	pH (4.59±0.02), 303 K, simulated zinc sulfate solution, concentration: 20−200 mg/L	23.04	[25]
Artificial zeolite	pH=6.5,298K, aqueous solutions, concentration: 3 mg/L	57.8	[26]
Artificial Zr-zeolite	pH=6.5,298K, aqueous solutions, concentration: 3 mg/L	128.2	This work

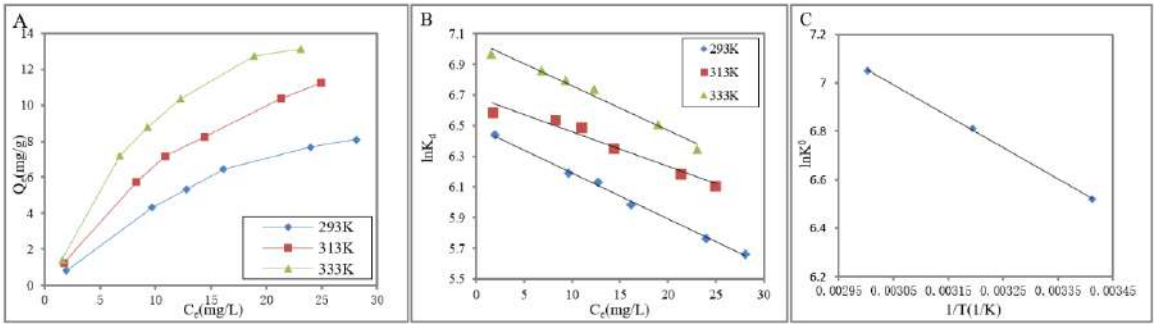

Fig. 5: The effect of temperature on the adsorption capacity of fluoride ion on AZZ. Initial pH=6.5, m/v=1g/L.

According to FIG. 5(A), it can be concluded that the adsorption capacity increased along with the temperature, implying that increasing temperature is beneficial for fluoride adsorption by AZZ in water.

The variation of standard free energy change (ΔG^0) can be computed based on equation (8):

$$\Delta G^0 = -\mathrm{R}T ln K^0 \quad (8)$$

where R is the universal gas constant (8.314 J·mol-1·K^{-1}), and T is the Kelvin temperature. K^0 is the adsorption equilibrium constant. $\ln K^0$ can be obtained by graphing $\ln K_d$ against C_e and deducing C_e to zero. Fig. 5(B) depicts the linearity plot of $\ln K_d$ with C_e for the adsorption of F^- on AZZ at 293, 313, and 333 K. Fig. 5(C) shows the linearizing plot of $\ln K^0$ versus 1/T. The variations in standard enthalpy (ΔH^0) and standard entropy (ΔS^0) are then deduced from the linearizing fit of $\ln K^0$ to 1/T in the following relationship equation (9):

$$\ln K^0 = \frac{\Delta S^0}{R} - \frac{\Delta H^0}{RT} \quad (9)$$

The thermodynamic values are listed in Table-3. This shows that the entropy change ΔS^0 =91.1 J mol^{-1}K^{-1}, the enthalpy change ΔH^0 =10.80 kJ mol^{-1}, and the standard free energy change ΔG^0= -15.89 kJ mol^{-1} at 293 K, -17.71 kJ mol^{-1} at 313 K, and -19.53 kJ mol^{-1} at 333 K. The positive result indicates that F^- adsorption on the AZZ surface is an endothermic procedure, and the negative standard free energy change indicates that F^- adsorption is a spontaneous procedure.

Effect of pH value on F^- adsorption

The pH value of the fluoride solution is among the necessary factors affecting the adsorption performance of the adsorbent because pH can affect not only the distribution of the charge in water but also the degree of ionization of the adsorbent. The impact of pH on F^- adsorption on AZZ in water is

demonstrated in FIG. 6. Based on Fig. 6, the adsorption of fluoride ions is responsive to changes in pH. The adsorption capacity drops sharply as the pH value increases above 4, decreases slightly between pH 5 to 10. The reduction in adsorption capacity at basic pH may be caused by the repulsive force of the AZZ negatively loaded surface with fluorine ions [27].

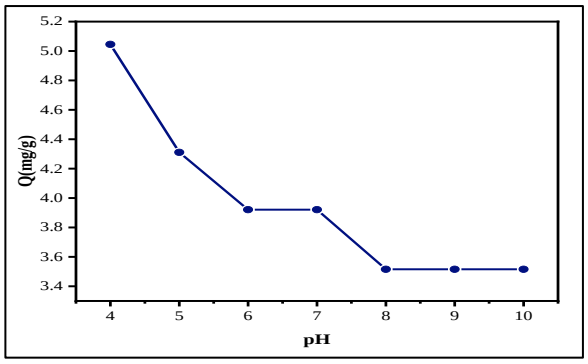

Fig. 6: The effect of initial pH on the amount of F^- absorbed on AZZ. $[F^-]_{initial}$=14ppm, m/v=1g/L, 298K.

Regeneration experiments

Five rounds of regeneration experiments were carried out with saturated alum as the regenerant, and the adsorption volume of AZZ for fluoride before and after regeneration is plotted in Fig. 7. After the first regeneration, the adsorption capacity remained essentially unchanged at 3.92 mg/g. No significant decrease in adsorption capacity was observed after five regeneration cycles, which remained at 78%. In addition, the regeneration procedure was convenient and time-efficient, as each regeneration took only one minute.

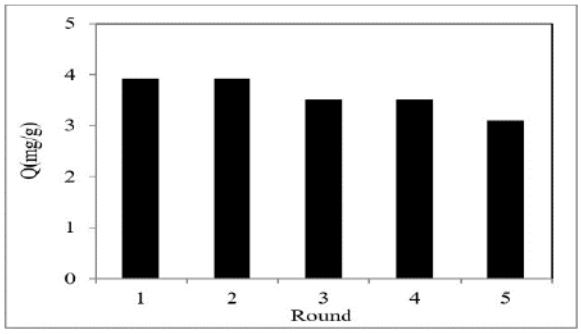

Fig. 7: Adsorption histogram of AZZ regeneration experiments. m/v=1g/L, initial pH=6.5, [F-]initial=20ppm, 298K; regeneration agent was saturated alum solution.

Adsorption mechanism

It is well known that the AZ surface is covered with hydroxyl groups, which can electrostatically attract anions, including F^-[28]. The zirconium modification on AZ resulted in the generation of zirconium oxides on AZ (Fig. 2 (B)). On the surface of zirconium metal oxides, hydroxylated surfaces are also formed by coordination with water in aqueous solution due to the unsaturated coordination of surface ions [29]. In general, the zeta potential of the solid surface in aqueous solution can reflect the electrostatic adsorption properties of solids in water. The zeta potentials of AZZ were determined at various pH values at ambient temperature (Fig. 8). In the pH region of 4.0-7.3, the zeta potential was positive, while in the pH range of 7.3-10, the zeta potential was negative. The surface of AZZ is charged positively in water at the environmentally correlated neutral or acid pH region, facilitating the adsorption of negatively charged F. Therefore, the electrostatic attraction between AZZ and F^- should be the important mechanism for F^- adsorption on AZZ.

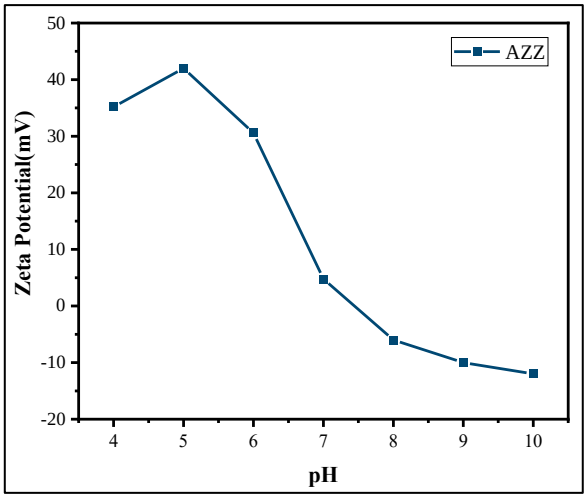

Fig. 8: Zeta potential of AZZ in water with different pH values.

Table-4: The derived thermodynamic parameters for zeolite adsorption of F^-

Adsorbents	T	ΔH^0(kJ/mol)	ΔS^0(J/(mol-K))	ΔG^0(kJ/mol)
AZZ	293	10.80	91.1	-15.89
	313			-17.71
	333			-19.53

Conclusion

AZ and AZZ were synthesized successfully in this work and were characterized by SEM and XRD analysis, which showed that AZZ was a composite of

AZ and ZrO_2 particles. The adsorption kinetics of fluoride by AZ and AZZ in water were very compatible with a pseudo-second-order kinetic model. Based on the isothermal data, the Langmuir model fitted better than the Freundlich model. The largest adsorption capacity of fluoride on AZZ reached up to 128.2 mg/g. Thermodynamic research proved that the adsorption procedure was an endothermic and spontaneous process. The utilized AZZ could be rejuvenated with an alum solution within one minute, and the adsorption capacity stood at 78 % after five cycles of regeneration. Because of its excellent adsorption capacity and regeneration performance, AZZ is a promising defluoridation material in water. The electrostatic attraction was deduced to be the important mechanism for F^- adsorption onto AZZ.

Acknowledgements

This work was supported by the Natural Science Foundation of Anhui Province (2008085MB57), Natural Science Research Key Project from Education Department of Anhui Province (KJ2021A0626) and Equipment & Demonstration Project for Chemical Remediation of Organic Contaminated Soil and Groundwater in Low Permeability Strata by Insitu Injection Method (HYB20230209).

References

1. Z. Zhang, Y. Tan and M. Zhong, Defluorination of wastewater by calcium chloride modified natural zeolite, *Desalination,* **276**, 252 (2011).
2. A. Teutli-Sequeira, V. Martínez-Miranda, M. Solache-Ríos and I. Linares-Hernández, Aluminum and lanthanum effects in natural materials on the adsorption of fluoride ions, *J. Fluorine Chem.,* **148**, 13 (2013).
3. Y. Sun, Q. Fang, J. Dong, X. Cheng and J. Xu, Removal of fluoride from drinking water by natural stilbite zeolite modified with Fe(III), *Desalination,* **277**, 127 (2011).
4. A. Bhatnagar, E. Kumar and M. Sillanpää, Fluoride removal from water by adsorption—A review, *Chem. Eng. J.,* **171**, 840 (2011).
5. X. Borgohain, A. Boruah, G. K. Sarma and M. H. Rashid, Rapid and extremely high adsorption performance of porous MgO nanostructures for fluoride removal from water, *J. Mol. Liq.,* **305**, 112799 (2020).
6. M. F. Chang and J. C. Liu, Precipitation Removal of Fluoride from Semiconductor Wastewater, *J. Environ. Eng.,* **133**, 425 (2007).
7. R. Kumar, P. Sharma, R. Singh and D. A. Aman, Equilibrium sorption of fluoride on the activated alumina in aqueous solution, *Desalin. Water Treat.,* **197**, 236 (2020).
8. C. C. Liu and J. C. Liu, Coupled precipitation-ultrafiltration for treatment of high fluoride-content wastewater, *J. Taiwan Inst. Chem. E.,* **58**, 263 (2016).
9. R. Simons, Trace element removal from ash dam waters by nanofiltration and diffusion dialysis, *Desalination,* **89**, 341 (1993).
10. N. Kabay, O. Arar, S. Samatya, U. Yüksel, and M. Yüksel, Separation of fluoride from aqueous solution by electrodialysis: Effect of process parameters and other ionic species, *J. Hazard. Mater.,* **153**, 113 (2008).
11. C. S. Sundaram and S. Meenakshi, Fluoride sorption using organic–inorganic hybrid type ion exchangers, *J. colloid interf. sci.,* **333**, 62 (2009).
12. J. He, Y. Yang, Z. Wu, C. Xie, K. Zhang, L. Kong and J. Liu, Review of fluoride removal from water environment by adsorption, *J. Environ. Chem. Eng.,* **8**, 104516 (2020).
13. C. Guan, Z. Xu, H. Zhu, X. Lv, and Q. Liu, Insights into the mechanism of fluoride adsorption over different crystal phase alumina surfaces, *J. Hazard. Mater.*, **423**, 127109 (2022).
14. B. E. Reed and M. R. Matsumoto, Modeling Cadmium Adsorption by Activated Carbon Using the Langmuir and Freundlich Isotherm Expressions, *Sep. Sci. Technol.,* **28**, 2195 (1993).
15. L. Jossens, J. M. Prausnitz, W. Fritz, E. U. Schlünder and A. L. Myers, Thermodynamics of multi-solute adsorption from dilute aqueous solutions, *Chem. Eng. Sci.,* **33**, 1106 (1978).
16. A. M. Raichur and M. J. Basu, Adsorption of fluoride onto mixed rare earth oxides, *Sep. Purif. Technol.,* **24**, 127 (2001).
17. Yu Wang, N. P. Chen, WEI Wei, CUI Jing, WEI Zheng-gui. Enhanced adsorption of fluoride from aqueous solution onto nanosized hydroxyapatite by low-molecular-weight organic acids, *Desalination.,* **276**, 161 (2011)
18. S I Alhassan , H. Wang , Y. He , *et al*. Fluoride remediation from on-site wastewater using optimized bauxite nanocomposite (Bx-Ce-La@500): Synthesis maximization, and mechanism of F^- removal, *J Hazard Mater.,***430**, 128401 (2022).
19. F. Morante-Carballo, N. Montalván-Burbano, P. Carrión-Mero and K. Jácome-Francis, Worldwide Research Analysis on Natural Zeolites as Environmental Remediation Materials, *Sustainability,* **13**, 6378 (2021).

20. Y. Wu, S. Zhang, X. Guo and H. Huang, Adsorption of chromium(III) on lignin, *Bioresource Technol.,* **99**, 7715 (2008).
21. I. Langmuir, The Constitution and Fundamental Properties of Solids and Liquids. Part I. Solids, *J. Am. Chem. Soc.,* **38**, 2295 (1916).
22. F. F. Fondeur, D. T. Hobbs, S. D. Fink and M. J. Barnes, Sorption Modeling of Strontium, Plutonium, Uranium, and Neptunium Adsorption on Monosodium Titanate, *Sep. Sci. Technol.,* **40**, 592 (2005).
23. A. Gunay, E. Arslankaya and I. Tosun, Lead removal from aqueous solution by natural and pretreated clinoptilolite: Adsorption equilibrium and kinetics, *J. Hazard. Mater.,* **146**, 371 (2007).
24. Barathi M, Kumar A S, Rajesh N. A novel ultrasonication method in the preparation of zirconium impregnated cellulose for effective fluoride adsorption, *Ultrasonics Sonochemistry.,***21**, 1090 (2014).
25. Y. Lai , Y. Kai , Y. Chao , *et al*. Thermodynamics and kinetics offluoride removal from simulated zinc sulfate solution by La(III)-modified zeolite,*T*
26. Fang, X., *et al*., Fluoride Adsorption On Artificial Zeolite In Water. *Fresenius Environmental Bulletin.,* **27**, 9739 (2018).
27. A. Salifu, B. Petrusevski, K. Ghebremichael, L. Modestus, R. Buamah, C. Aubry and G. L. Amy, Aluminum (hydr)oxide coated pumice for fluoride removal from drinking water: Synthesis, equilibrium, kinetics and mechanism, *Chem. Eng. J.,* **228**, 74 (2013).
28. A. Chakraborty and M. K. Naskar, Sol–gel synthesis of alumina gel@zeolite X nanocomposites for high performance water defluoridation: batch and column adsorption study, *Mater. Adv.,* **3**, 8556 (2022).
29. M. S. Onyango, Y. Kojima, O. Aoyi, E. C. Bernardo and H. Matsuda, Adsorption equilibrium modeling and solution chemistry dependence of fluoride removal from water by trivalent-cation-exchanged zeolite F-9, *J. colloid interf. sci.,* **279**, 350 (2004).